EFDA–JET–CP(13)02/03

AL. Campergue, P. Jacquet, V. Bobkov, D. Milanesio, I. Monakhov, L. Colas,
G. Arnoux, M. Brix, A. Sirinelli and JET EFDA contributors

Characterization of Local Heat Fluxes around ICRF Antennas on JET

Characterization of Local Heat Fluxes around ICRF Antennas on JET

AL. Campergue[1], P. Jacquet[2], V. Bobkov[3], D. Milanesio[4], I. Monakhov[2], L. Colas[5], G. Arnoux[2], M. Brix[2], A. Sirinelli[2] and JET EFDA contributors*

JET-EFDA, Culham Science Centre, OX14 3DB, Abingdon, UK

[1]Ecole Nationale des Ponts et Chaussées, F77455 Marne-la-Vallée, France
[2]EURATOM-CCFE Fusion Association, Culham Science Centre, OX14 3DB, Abingdon, OXON, UK
[3]Max-Planck-Institut für Plasmaphysik, EURATOM-Assoziation, Garching, Germany
[4]Politecnico di Torino, Department of Electronics, Torino, Italy
[5]CEA, IRFM, F-13108 Saint-Paul-Lez-Durance, France
** See annex of F. Romanelli et al, "Overview of JET Results", (24th IAEA Fusion Energy Conference, San Diego, USA (2012)).*

Preprint of Paper to be submitted for publication in Proceedings of the 20th Topical Conference on Radio Frequency Power in Plasmas, Sorrento, Italy.
25th June 2013 - 28th June 2013

ABSTRACT.
When using Ion Cyclotron Range of Frequency (ICRF) heating, enhanced power deposition on Plasma-Facing Components (PFCs) close to the antennas can occur. Experiments have recently been carried out on JET with the new ITER-Like-Wall (ILW) to characterize the heat fluxes on the protection of the JET ICRF antennas, using Infra-Red (IR) thermography measurement. The measured heat flux patterns along the poloidal limiters surrounding powered antennas were compared to predictions from a simple RF sheath rectification model. The RF electric field, parallel to the static magnetic field in front of the antenna, was evaluated using the TOPICA code, integrating a 3D flattened model of the JET A2 antennas. The poloidal density variation in front of the limiters was obtained from the mapping of the Li-beam or edge reflectometry measurements using the flux surface geometry provided by EFIT equilibrium reconstruction. In many cases, this simple model can well explain the position of the maximum heat flux on the different protection limiters and the heat-flux magnitude, confirming that the parallel RF electric field and the electron plasma density in front of the antenna are the main driving parameters for ICRF-induced local heat fluxes.

HEAT FLUXES ON LIMITERS
When ICRF heating is used on JET, hot spots can develop on the limiters surrounding active antennas [1]. Maximum deposited heat fluxes (Q_{dep}) of 4.5 MW/m^2 were recently observed in JET-ILW [2], justifying the need for modelling of these RF specific heat loads. For these studies, a series of discharges were performed, where only half of an antenna viewed by the IR camera was used in order to simplify the analysis of the heat-load pattern: straps 3 and 4 of antenna A (Fig.1). In this case, large variations of the surface temperature are measured on the "1D" Poloidal limiter (PL), on the bottom of the septum in the middle of the antenna and on the "2D" PL. Experimental heat fluxes were evaluated from IR temperature measurements via two different methods: a deconvolution method [1], using a linear inversion process which involves the definition of a thermal response of the object; and computation using the Theodor code [3], which solves the heat diffusion equation with temperature dependant conduction coefficient and heat capacity. These two approaches gave similar results. The parallel heat flux (heat flux along static magnetic field lines) $Q_{//}$ was evaluated from the deposited heat-flux as follow: $Q_{\|} = \frac{Q_{dep}}{\cos(\theta_n)}$ where θ_n is the angle between the magnetic field lines and the vectors perpendicular to the limiter's surface. Examples of measured heat flux maps for different limiters around antenna A are shown in Fig.2 where the x axis is the toroidal angle in radian and the y-axis is the vertical altitude z. The measured heat flux at the toroidal positions indicated by the white rectangles in Fig.2 (corresponding to maximum values) was compared to the calculations from a RF sheath rectification model. comparison with rf sheaTh rectification model
A simple RF sheath rectification model [4] was used for this study: $Q_{\|} = eZV_{DC}$ where e is the elementary charge, Z is the atomic number of plasma ions (pure deuterium assumed), n is the electron density, $c_s = \left(\frac{k(T_e + T_i)}{m_i}\right)^{1/2}$ the local sound speed in the plasma, (assumed $T_e = T_i = 20$eV) and $V_{DC} = \frac{1}{\pi}\left|\int E_{\|} dl\right|$ is the RF rectified sheath potential. $E_{//}$ is the RF electric field parallel to the

static magnetic field in front of the antenna; it was evaluated using the TOPICA code [5] which uses a 3D flattened model of the antenna. The field intensity is scaled to the launched ICRF power corresponding to the experience (1MW for Pulse No: 83063 and 0,75MW for Pulse No: 83065, both discharges with $B_t = 2.4$T, $I_p = 2$MA, $f_{ICRF} = 42$MHz, N = 1 (H)D heating scenario). The parallel electric field is integrated along straight magnetic field lines passing in front of the antenna to the point where they reach the limiter. The tilt angle is 10.5°. $E_{//}$ is calculated at 2.3cm in front of the Faraday Screen, at the plasma vacuum interface of the TOPICA antenna model.

The integration zone of $E_{//}$ to calculate V_{DC} was adapted to the type of limiter analyzed: for the 1D (resp. 2B) limiter, the integration path covers the Left Hand Side (LHS) of the TOPICA calculation domain (resp. Right Hand Side -RHS for 2B) as indicated in solid lines (resp. dashed lines) in Fig.3. As the 2D limiter is out of the calculation domain for $E_{//}$ in TOPICA, the results of the integration were projected to the limiter structure taking into account the tilt angle of the field lines. The integration path was slightly different for the septum. For the top part of the septum ($z > 0$), the integration path was on the RHS of the septum, and for $z < 0$, the integration path was on the LHS, coherently with the topology of the field lines impinging on the limiters.

The density at the limiters was evaluated using two diagnostics: a Li-beam diagnostic [6] and an edge reflectometry diagnostic [7]. The density measurements were mapped along the vertical position at the limiters using the magnetic field 2D map from the EFIT equilibrium solver [8]. Consistently with the fact that the curvature of the plasma is larger than the curvature of the outer poloidal limiters, the density peaks at z~0.1m (see Fig.4) where the distance between the plasma and the limiter is at minimum.

The heat fluxes from IR thermography along the poloidal limiters 1D and 2D are plotted as a function of vertical height and compared to the estimates from the RF sheath model in Fig.5. Two antenna strap phasings were used: $-\pi/2$ for Pulse No: 83063 and π (dipole) for Pulse No: 83065. From Fig.5, one can conclude that the model (solid and dashed grey lines) can well reproduce the heat flux pattern on the 1D and 2D poloidal limiters and also on the antenna septum (not shown). It is important to take into account the dependence of n with the vertical position on the limiters to accurately predict the heat flux pattern; on Fig.5(a), the dashed black line shows V_{DC} only with peaks at $z \sim -0.8$m and $z \sim +0.9$m which are not observed in the measured heat pattern. The heat fluxes magnitude is also correctly predicted given the uncertainties in n measurements in the Scrape-Off-Layer (SOL). In agreement with the measurements, the model also predicts a lower magnitude in the heat flux when changing the antenna phasing from $-\pi/2$ to dipole.

The same analysis was also carried out for the 2B limiter. In this case, the measured heat fluxes are importantly reduced w.r.t the other limiters and w.r.t the predictions from the model. A possible cause is the shadowing of this particular limiter which results in a local reduction of the density, stressing again the importance of local plasma parameters in driving RF specific heat deposition.

CONCLUSIONS

For most cases, the simple RF sheath rectification model presented in this paper with $E_{//}$ calculated using the TOPICA antenna modeling code can predict accurately the heat flux pattern along the poloidal limiters surrounding the powered antenna and the heat flux magnitude. The model is also consistent with the observed reduced intensity when the strap phasing changes from $-\pi/2$ to dipole. We also stress-out the importance of the local SOL properties in front of the powered antennas. To go further in the analysis of these RF specific heat-fluxes, it will be important to get reliable SOL measurements, as far is practically feasible, in front of the antennas. These will help understanding how ICRF power can locally modify the SOL properties [9, 10], which together with advanced RF sheath rectification models [11] will be instrumental in the optimization of ICRF antennas for next fusion devices.

ACKNOWLEDGMENTS

This work, part-funded by the European Communities under the contracts of Association between EURATOM and CCFE, was carried out within the framework of the European Fusion Development Agreement. The views and opinions expressed herein do not necessarily reflect those of the European Commission. This work was also part-funded by the RCUK Energy Programme under grant EP/I501045.

REFERENCES

[1]. P. Jacquet, *et al.,* Nuclear Fusion **51** (2011) 103018 (16pp)
[1]. P. Jacquet, *et al*., Journal of Nuclear Materials **438** (2013) S379–S383
[1]. A. Herrmann, *et al*., *Plasma Physics and Controlled Fusion,* **37**, 17-29 (1995)
[1]. L. Colas*, et al*., Nuclear Fusion **46** (2006) S500–13
[1]. D. Milanesio, *et al*., Nuclear Fusion **49** 115019 (2009)
[1]. M. Brix, *et al*., Review of Scientific Instruments, **81** (2010), 10D734
[1]. A. Sirinelli, *et al.,*Review of Scientific Instruments, **81** (2010), 10D939
[1]. L.L Lao, **et al**., 1990 Nuclear Fusion **30** 1035
[1]. M. Becoulet, *et al*., Physics of Plasmas (2002) **9** 2619–32
[1]. Dirk Van Eester, Kristel Crombé and Volodymyr Kyrytsya. Plasma Phys. Control. Fusion **55** (2013) 025002
[1]. J. Jacquot, *et al.*, Radio-frequency Sheath Physics / Experimental Characterization on Tore Supra and Related Self-consistent Modeling, these proceedings

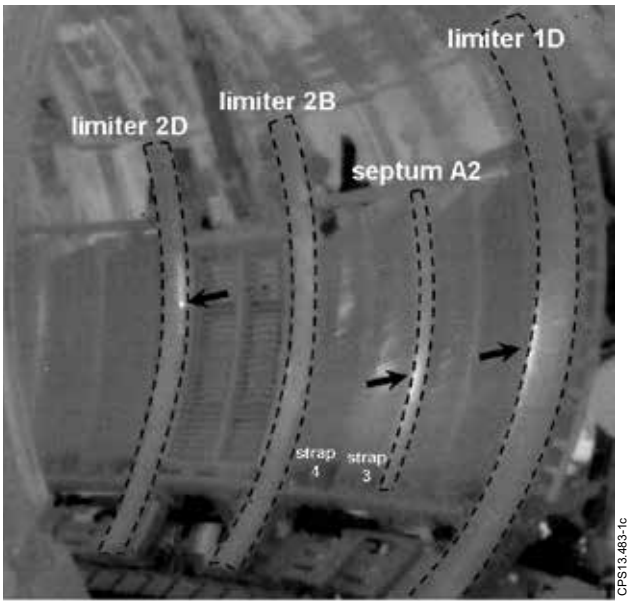

Figure 1: JET Pulse No: 83063 t = 13.0s, IR frame showing locations where ICRF hot spots are observed when powering straps 3 and 4 of antenna A.

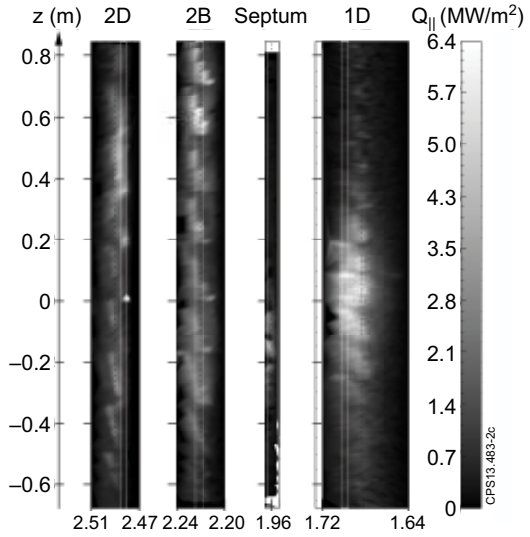

Figure 2: JET Pulse No: 83063 t = 13.0s. Heat flux maps on the limiters 2D and 2B, on the antenna A septum and on 1D (from left to right). The x axis is the toroidal angle (in radians) the y-axis is the vertical position. White rectangles show the zone selected for comparison with modeling.

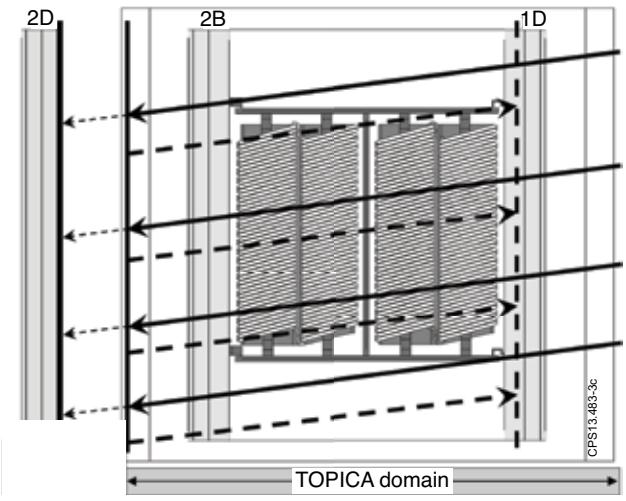

Figure 3: TOPICA flattened model of tFhe ICRF antenna. The dotted arrows show the integration domain for the limiter 1D, and the full arrows for the limiter 2D.

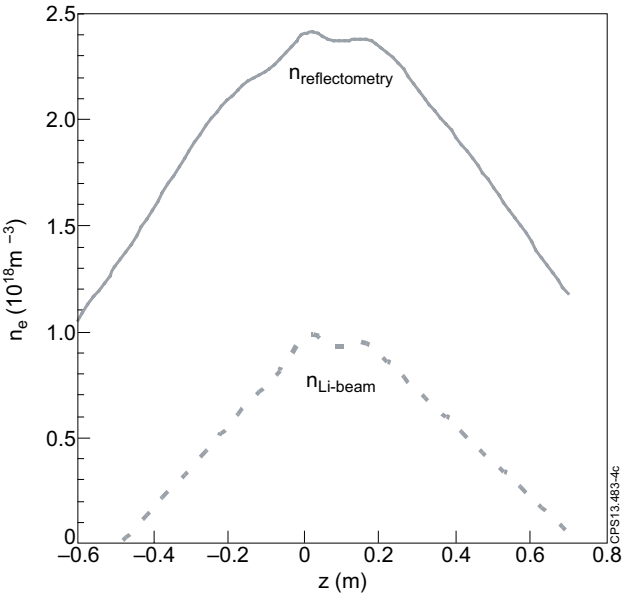

Figure 4: JET Pulse No: 83063 t = 13s. Density profile mapped along the limiter, with the edge reflectometry diagnostic (full grey) and the Li-beam (dashed grey).

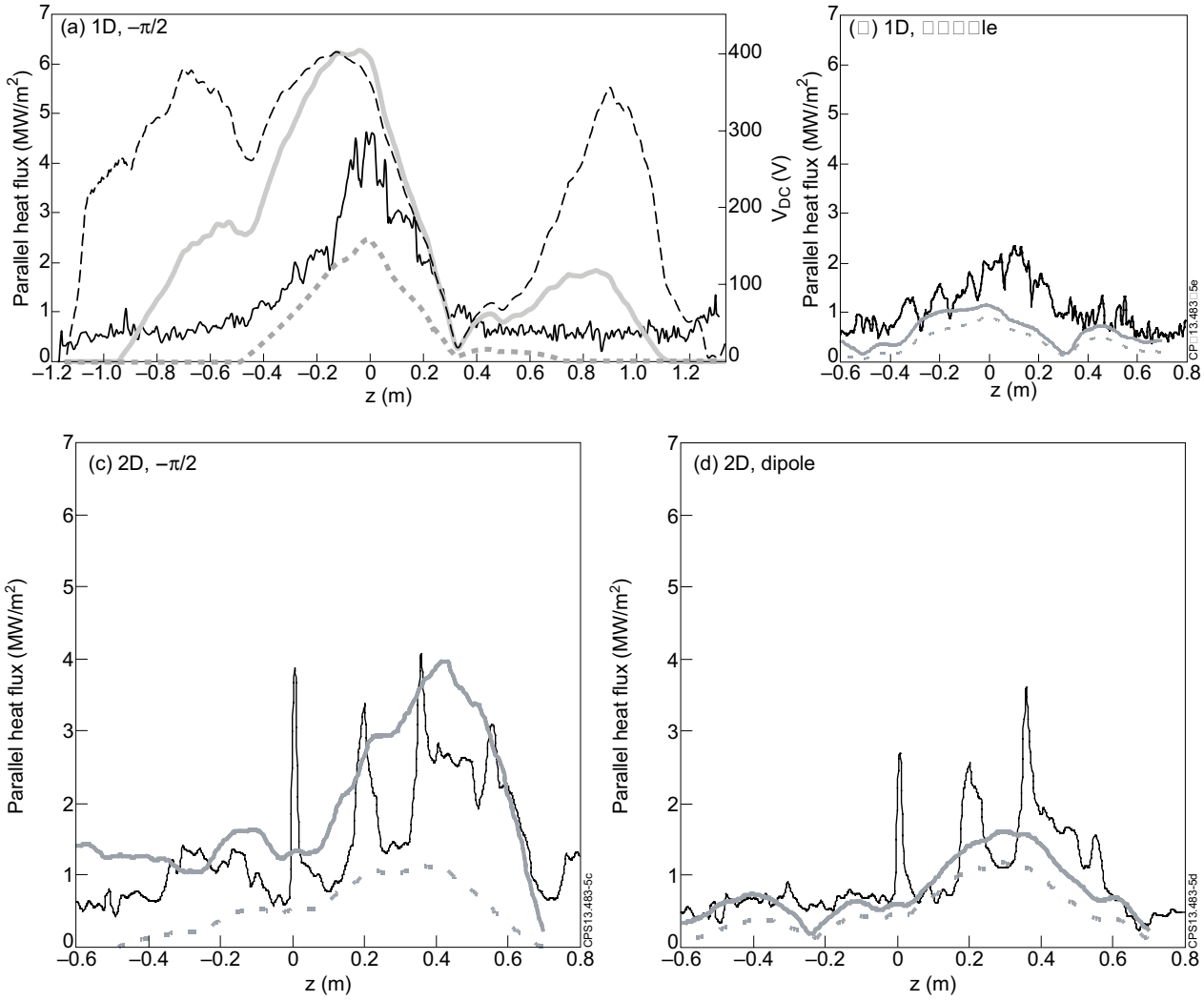

Figure 5: Comparison of the parallel heat fluxes measured via IR and predicted using the model. Two different pulses are studied: JET Pulse No: 83063 with –π/2 phasing and JET Pulse No: 83065 with dipole phasing, both at t = 13s. Graphs (a) and (b) are for the limiter 1D and graphs (c) and (d) for the limiter 2D.